Selective attention modifies weights of distinct visual signals in human decision making

Authors: Dragan Rangelov[a] and Jason B. Mattingley[a,b,c]

Affiliations:

[a]Queensland Brain Institute, The University of Queensland, St Lucia, QLD 4072, Australia

[b]School of Psychology, The University of Queensland, St Lucia, QLD 4072, Australia

[c]Canadian Institute for Advanced Research (CIFAR)

Corresponding Author:

Dragan Rangelov

ORCID: 0000-0001-7648-6447

Post: Queensland Brain Institute

The University of Queensland

St Lucia, QLD 4072, Australia

Phone: +61 401 281 181

Email: d.rangelov@uq.edu.au

Keywords: selective attention, decision-making, electroencephalography, mixture distribution modelling

Abstract

The ability to decide on the basis of multiple goal-relevant signals while ignoring distractors is a hallmark of adaptive, intelligent behaviour. While attention and decision-making processes have been well characterised in isolation, little is known about how the two interact. To independently manipulate task relevance and information integration, we presented moving dots in both a cued (target) colour and an uncued (distractor) colour. Using electroencephalography, we recorded brain activity in human observers as they reproduced the average motion direction of two consecutively presented targets. Although completely spatially intermingled with the targets, the distractors had remarkably little influence on either behavioural or electrophysiological correlates of decision-making. Consistent with this, we found only target-related processing in a follow-up experiment which used frequency-tagging to individually monitor target and distractor processing. Our findings suggest that two task-relevant stimuli can be efficiently combined to inform decision-making, implying a previously undocumented coupling between attention and decision-making.

Introduction

Cognition can be conceived of as a cascade of processes, beginning with the encoding of sensory input and ending with appropriate behavioural choices. Sequential-sampling decision-making models (Forstmann, Ratcliff and Wagenmakers, 2016; Ratcliff *et al.*, 2016) have had considerable success in describing choice behaviour in terms of both behavioural performance and neural activity. According to these models, decision-making relies on a central decision variable, an abstract quantity that accumulates in time toward one of several possible choice alternatives. On these accounts, a choice is made once the decision variable reaches threshold. In one widely employed decision-making task – the random-dot motion discrimination task (Shadlen and Kiani, 2013; Ratcliff *et al.*, 2016) (see Fig. 1a) – participants are shown fields of randomly moving dots and are asked to judge the motion direction of a fraction of the dots that move coherently. Studies in both animals (Shadlen and Kiani, 2013) and humans (Heekeren, Marrett and Ungerleider, 2008; Ratcliff, Philiastides and Sajda, 2009; O'Connell, Dockree and Kelly, 2012; Kelly and O'Connell, 2013; Twomey, Kelly and O'Connell, 2016) have shown that neural activity recorded during random-dot motion discrimination follows a trajectory that resembles the accumulation of a decision variable, thereby lending neurobiological support to sequential-sampling decision-making models.

To date, much has been learned (Summerfield and Tsetsos, 2015; Spitzer, Waschke and Summerfield, 2017) about simple perceptual decision-making in humans and other animal species. In the real world, however, decisions are often more complex, requiring judgements on stimuli that are separated in time and space, and which may or may not be

task relevant. For example, deciding to cross a busy road requires us to integrate the motion directions of vehicles coming from both the left and right sides, while disregarding any movements made by people or objects on the sidewalk. Little is known about how the brain regulates decision-making when it receives competing – task-relevant and irrelevant – sensory inputs. With a single, task-relevant dot-motion patch, integrating all dot trajectories is clearly the optimal approach as it would yield strongest noise suppression. It remains unclear, however, how efficiently observers can integrate only a task-relevant *subset* of dots from amongst a spatially overlapping field of task-irrelevant stimuli. In this scenario, integrating all dot trajectories is clearly suboptimal as the net motion direction would be the average of both the relevant and irrelevant signals. To discern the task-relevant motion direction, selectively attending to task-relevant visual input would be necessary. Despite the critical role of attention for accurate decisions, most work on decision-making to date has used only task-relevant dot patches. In the current study we characterised the behavioural and neural mechanisms via which attention regulates complex perceptual decision-making.

To investigate whether and to what extent task-irrelevant, distractor signals influence decision-making, we used random-dot displays (Fig. 1a) comprising *two* intermingled dot patches moving in different directions at supra-threshold coherence. The two patches had different colours, with one having a cued (target) colour and the other an uncued (distractor) colour. As recent studies have suggested that task demands may influence decision-making (Churchland, Kiani and Shadlen, 2008; Leite and Ratcliff, 2010; Tsetsos, Usher and McClelland, 2011; Churchland and Ditterich, 2012; Loughnane *et al.*, 2016; Li *et al.*, 2017; Spitzer, Waschke and Summerfield, 2017), we cued participants, in

separate blocks of trials, to monitor either for a single target colour across epochs, or for each of two different target colours.

To investigate integration of individual decisions over time, we measured behavioural and neural responses while participants performed a novel, complex decision-making task. We presented *two* epochs of target motion per trial and observers had to reproduce the average target motion direction. This averaging task enabled us to characterise the integration of two simple decisions into one, complex decision. Participants' reproduction errors provided a continuous index of decision accuracy, which we analysed using computational modelling, as described below, to quantify the unique contributions of target and distractor events to the final decision. In addition, the averaging task allowed us to dissociate decision-making from response selection and execution processes, as the stimuli were orthogonal to the final response in this task.

Results

In Experiment 1, a group of 36 participants judged average motion direction across three successive epochs within each trial (Fig. 1a). Participants were instructed to monitor the motion direction of the target-coloured patches, and ignore the distractor-coloured patches. Two, randomly selected epochs contained concurrent target and distractor motion patches, while a third epoch contained two distractor patches. To quantify task performance, we computed error magnitudes (Fig. 1b) by subtracting the true average motion direction from the reproduced direction. The distributions of error magnitudes per experimental condition were used to estimate the response precision (K) and guessing rates (α), which reflect how well participants performed the task and how often they guessed,

respectively. The average guessing rates (α) decreased significantly ($F_{1,32}$ = 5.56, p = .025, η_p^2 = .15) as attentional demands increased: $\alpha_{M/SEM}$ =.34/.05 and .28/.05 for one- and two-target colour conditions, respectively. The average response precision was high (one target colour: $K_{M/SEM}$ = 10.90/1.77, 41° full-width-at-half-maximum (FWHM); two colours: $K_{M/SEM}$ = 12.72/1.92, 38° FWHM) and did not differ significantly between conditions ($F_{1,32}$ = 1.39, p = .248). For reference, the average tuning width (Treue, Hol and Rauber, 2000) of individual neurons in macaque area MT is about 60° FWHM. The excellent behavioural performance of our participants demonstrates highly effective target selection from the concurrent and spatially interspersed distractors.

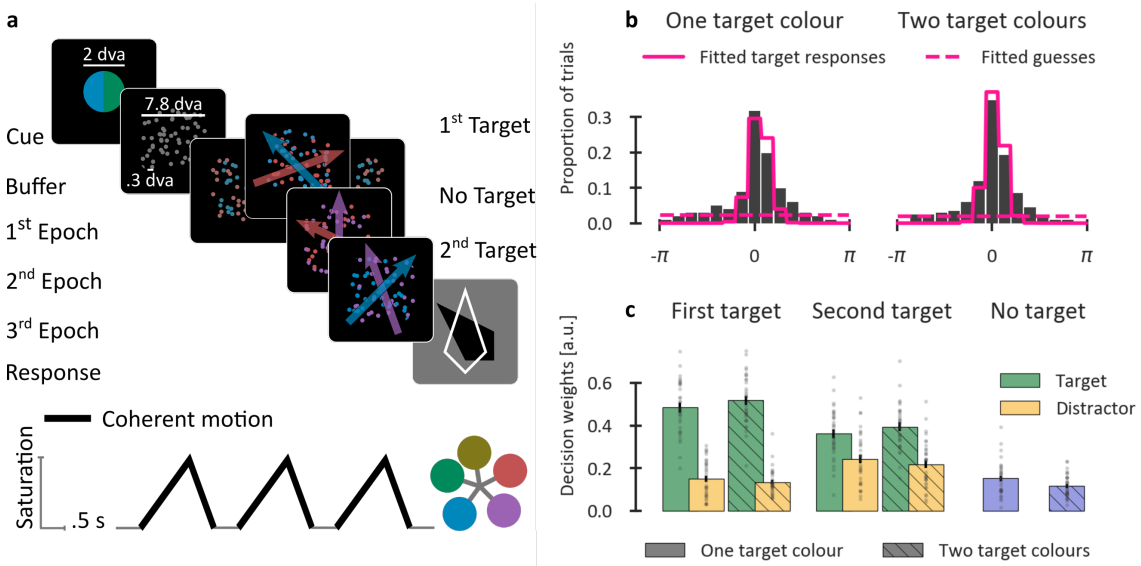

Figure 1. Schematic of the stimuli, task and the behavioural results in Experiment 1. a, Example stimulus sequence from a typical trial (above) together with the timing of colour saturation modulation and coherent-motion onsets (below). The cue indicated task-relevant (target) colours in that trial. Two, randomly selected, epochs of coloured dots comprised both target- and distractor-coloured dots (First and Second target), whereas the remaining epoch comprised only distractor-coloured dots (No Target). Participants had to reproduce the *average* motion direction of target-coloured dots by adjusting the orientation of a response dial

(black pointer) followed by a correct feedback within the same display (white pointer). **b**, Group-level histograms (bars) of the error magnitude (reproduced motion direction – expected) in Experiment 1, shown separately for one- and two-target colour trials. The lines show fitted distributions of target responses (full lines) and guesses (dashed lines) using mixture-distribution modelling of each individual participant's data. **c**, Average decision weights showing the contributions of each presented motion direction to the decision. The yellow and green bars denote decision weights for target and distractor motion, respectively. Since there were no significant differences ($t < 1$) between the two non-target motions in the "No target" condition (blue bars), only the average of the two is shown. Grey dots denote individual participants.

To quantify how much each of the presented target and distractor signals influenced observers' average-motion decisions, we used linear regression modelling with complex-valued data (see Methods). The decision weights (Fig. 1c) were much higher ($F_{2,64} = 326.80$, $p < .001$, $\eta_p^2 = .91$) for targets (.44/.01) than for either concurrently presented distractors (.19/.01) or distractors presented on their own (.13/.01), indicating efficient attentional selection of task-relevant signals. There was a reliable order effect with higher target weights for the first epoch than for the second (.50/.01 vs. .38/.02, $t_{32} = 4.74$, $p < .001$); analogously, distractor weights were lower for the first epoch than for the second (.14/.01 vs. .23/.01, $t_{32} = 4.68$, $p < .001$). Finally, the target weights were marginally higher for two target colours relative to one (.46/.01 vs. .42/.01, , $t_{32} = 2.14$, $p = .047$), while attentional demands had no effect on distractor weights ($t_{32} = 1.63$, $p = .113$).

We next analysed the dynamics of sensory and attentional processes feeding into decision-making stages. If attention mediates perception and decision-making, then neural correlates of attentional selection should be stronger for target-present than target-absent epochs. To characterise attentional selection, we measured the onset latency, peak

amplitude and slope of a recently described (Loughnane *et al.*, 2016) event-related potential (ERP) component, the N2b, which manifests as a bilateral negativity over posterior scalp sites.

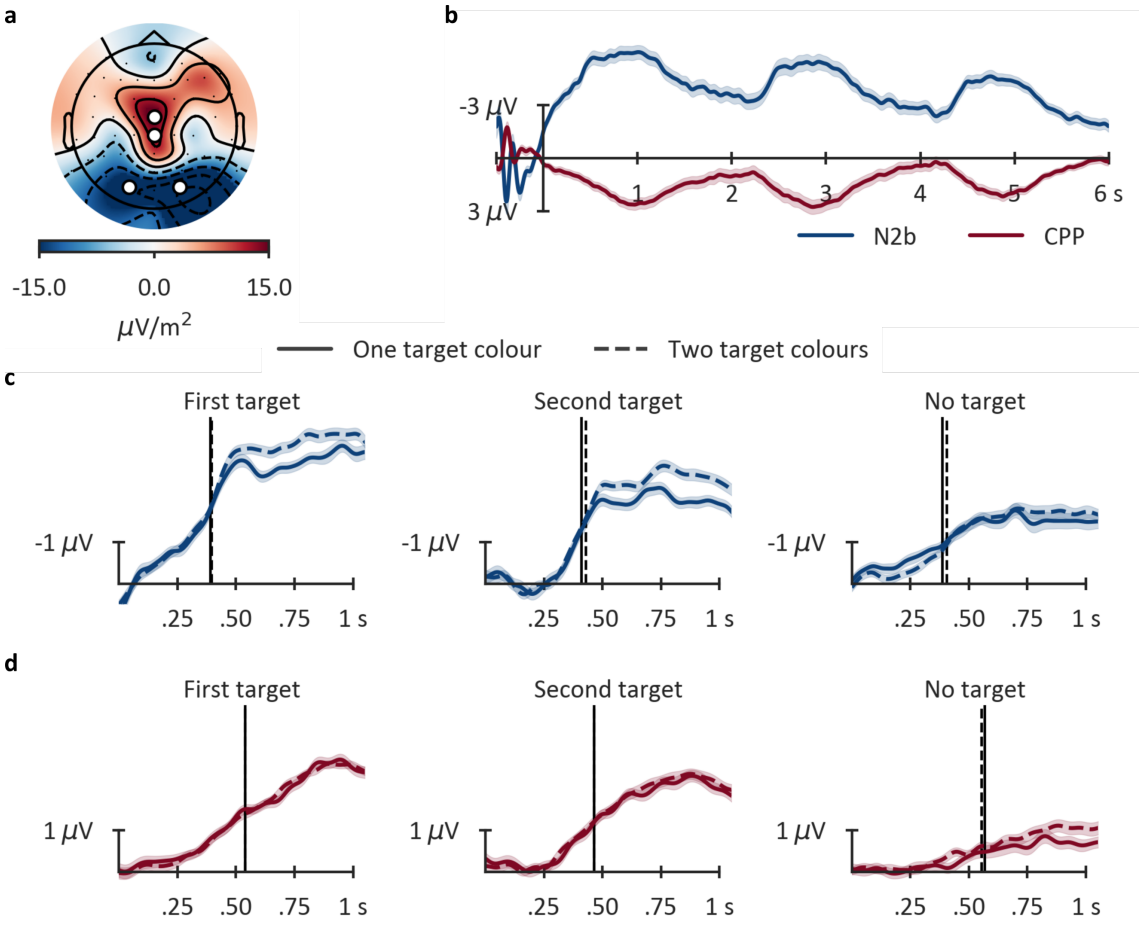

Figure 2. Time course of ERP correlates of attentional selection and decision making in Experiment 1. a, Surface-Laplacian-filtered EEG topography averaged across all conditions at times of peak colour saturation for all three epochs (1 s, 3 s, and 5 s after stimulus onset). The markers denote electrode pairs [O1 and O2] and [CPz and Cz] which were used for ERP analyses. **b**, Time-course of target selection (the N2b, blue trace) and decision-making (the CPP, red) ERPs averaged across all experimental conditions (M ± 1 within-participants SEM (Morey, 2008)) for the total trial duration. **c**, Time-course of the N2b ERP during the gradual increase in colour saturation, separately per epoch and experimental condition. **d**, Time-course of the CPP ERP during the

same period. For the purpose of data presentation, all traces were low-pass filtered at 10 Hz using a 4th order Butterworth IIR filter. Data analyses were conducted using unfiltered data.

Inspection of the ERP topographies (Fig. 2a) revealed a bilateral posterior negativity consistent with the N2b topography. The N2b time-traces (Fig. 2b) peaked at .7, 2.7, and 4.7 s, closely mirroring the modulation of colour saturation within each trial. The N2b onset latency (403 ms, Fig. 2c) was comparable across experimental conditions ($F_c < 1$), indicating that the modulation of colour saturation was registered irrespective of the colour's task-relevance or attentional demands. Task-relevance, by contrast, had a significant effect on the *slope* of the N2b ($F_{c(1,32)} = 3.58$, $p = .034$), with significantly steeper slopes for the target epochs (-11.82 μV/s and -11.55 μV/s for the first and second epoch, respectively, $t_{c(32)} < 1$) than for the no-target epoch (-4.02 μV/s). Mirroring the behavioural order effect, the N2b peak amplitude was higher for the first target epoch than for the second (-3.59 μV and -2.84 μV, respectively), and both were higher than the no-target epoch (-2.04 μV, all $t_{c(32)} \geq 3.46$, all $p < .001$). Also in line with the behavioural results, the robust differences between target- and no-target epochs suggest that only task-relevant sensory input is passed on to decision-making stages. Interestingly, increasing the attentional demands from one to two target colours did not affect N2b slopes ($F_c < 1$). This finding nicely complements recent reports (Eimer and Grubert, 2014; Grubert *et al.*, 2017) that spatial attention can be guided by two attentional templates (i.e., two target colours) just as efficiently as by one template (i.e., one colour). Here we go beyond this work by showing that similar mechanisms control not only spatial attention, but feature-based attention too. Critically, attentional demands influenced the peak N2b amplitude which was significantly lower for one target colour than for two (-2.69 and -2.96 μV, respectively, $F_{c(1,32)} = 4.96$, $p = .033$). Using a sequential-

173 sampling decision-making framework to interpret the N2b results, it appears that higher
174 attentional demands increased the decision threshold (as measured by the peak N2b
175 amplitude) for selecting the target colour, but did not affect the speed of evidence
176 accumulation (as measured by the N2b slope).

177 Next, we characterised the time-course of decision-making. If evidence accumulation
178 relies primarily on task-relevant signals, then neural correlates of evidence accumulation
179 should be stronger for target epochs relative to the no-target epoch. To characterise the
180 temporal dynamics of evidence accumulation, we quantified the onset latency, slope and
181 peak amplitude of an ERP known as the central-parietal positivity (CPP). Previous research
182 has shown that the time-course of the CPP closely resembles the time-course of evidence
183 accumulation: specifically, its amplitude builds up gradually (O'Connell, Dockree and Kelly,
184 2012), the build-up slope is proportional to stimulus quality (Kelly and O'Connell, 2013), and
185 it is observed even in the absence of overt responses (Twomey, Kelly and O'Connell, 2016).
186 Inspection of the ERP topographies (Fig. 2a) revealed a central-medial positivity consistent
187 with the usual CPP (O'Connell, Dockree and Kelly, 2012). Throughout the trial, the CPP (Fig.
188 2b) closely followed the time-course of colour modulation, with three distinct peaks
189 coinciding with the three episodes of maximum colour saturation. The onset latency (522
190 ms) and the CPP slope (3.31 μV/s) were similar across experimental conditions (all $F_c < 1$),
191 suggesting that the rate of evidence accumulation did not differ between epochs or
192 attentional demands. This is not entirely surprising, as the rate of evidence accumulation for
193 simple visual decisions has been shown to depend on motion coherence (Twomey, Kelly and
194 O'Connell, 2016), which was held constant in our paradigm. The peak CPP amplitude,

however, *decreased* between epochs ($F_{c(2,64)} = 46.41$, $p < .001$), from the first target epoch to the second epoch and then to the no target epoch (2.72, 2.44 and 1.10 μV, respectively, all $t_{c(32)} \geq 1.79$, $p \leq .041$).

Finally, attentional demands (one vs. two target colours) had no significant effect on the peak CPP amplitude, either as a main effect ($F_c < 1$) or in combination with epoch ($F_{c(2,64)} = 1.44$, $p = .244$). Overall, the CPP analyses revealed that the decision threshold (as indexed by the peak CPP amplitude) was sensitive to the presence of a target motion patch, suggesting that more sensory evidence was needed to reach a decision in target-present than in no-target epochs.

Taken together, the ERP results of Experiment 1 revealed reliable differences between target-present and no-target epochs for both the N2b and CPP components, suggesting that complex visual decision-making – here involving the averaging of two successive motion targets – relies on attentional selection of task-relevant stimuli. It remains unclear, however, in what way does visual attention influence the processing of concurrently presented target- and distractor-coloured signals: attention could boost target encoding, suppress distractor processing, or potentially influence both. The goal of Experiment 2 was to characterise how attention affects target and distractor processing in our novel decision-making task. To measure responses to targets and distractors independently, in Experiment 2 the dot fields corresponding to these two stimulus types flickered concurrently at different frequencies (12 and 18 Hz; see Methods). The introduction of these flickering displays yielded distinct, time-resolved steady-state evoked potentials (SSVEPs, see Norcia *et al.*, 2015). Using a similar approach, studies on visual

attention have shown (Andersen and Müller, 2010; Andersen, Müller and Hillyard, 2015) that when two differently-coloured, spatially overlapping random-dot patches are presented, electrophysiological responses to the task-relevant, target patch are stronger than those to concurrent distractor stimuli. Unlike previous studies, the modulation of colour saturation enabled us to track attentional deployment within a trial as a function of stimulus discriminability.

Experiment 2 differed from Experiment 1 in two further important ways (Fig. 3a). First, since we wished to focus on the processing of concurrently presented target and distractor colours, we removed no-target epochs and presented only target-present epochs. Second, to separate in time neural processes associated with selection of the target versus distractor colour from processes associated with motion processing, we first increased colour saturation within each epoch, and then presented the critical coherent motion events over a jittered interval during the period of maximum saturation. A new group of 36 participants took part in Experiment 2.

The behavioural results of Experiment 2 were strikingly similar to those of Experiment 1. Response precision (Fig. 3b) was high and comparable between the one- and two-target colour conditions (K/FWHM = 7.96/48° and 7.37/50°, $F_{1,30} = 2.37$, $p = .134$). Guessing rates were low and virtually identical for one and two target colours (.12 for both conditions, $F < 1$). Decision weights (Fig. 3c) for targets were seven times higher than those for distractors (.56/.01 and .08/.01, respectively, $F_{1,30} = 1{,}845$, $p < .001$, $\eta_p^2 = .98$). We also replicated the serial order effect, with higher decision weights for the first epoch than the second, both for targets (.58/.01 vs. .54/.01, $t_{30} = 3.06$, $p = .004$) and distractors (.09/.01 vs.

239 .07/.01, t_{30} = 3.32, p = .002). Finally, increasing attentional demands from one to two target

240 colours had no effect on decision weights, either as a main effect or in combination with the

241 other factors (all F ≤ 1.35, all p ≥ .254).

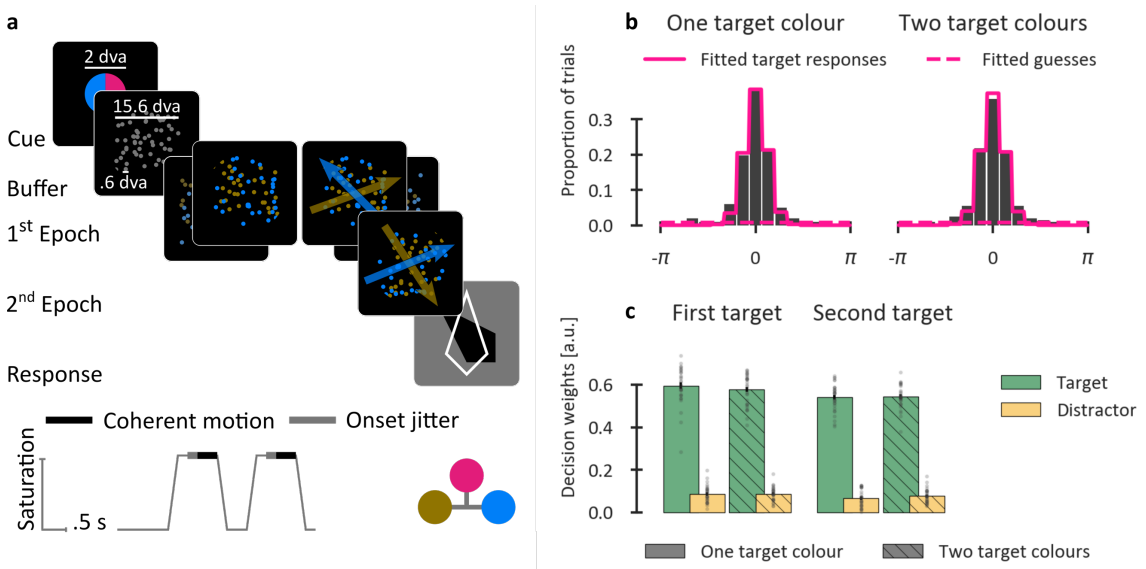

242

243 **Figure 3. Schematic of the stimuli, task and the behavioural results in Experiment 2. a,** Example stimulus

244 sequence from a typical trial (above) together with the timing of colour saturation modulation and coherent-

245 motion onsets (below). Only target-present epochs were presented, and the increase in colour saturation and

246 onset of coherent motion were separated in time. Dot patches were frequency-tagged at 12 and 18 Hz

247 (counterbalanced across target and distractor stimuli). **b**, Group-level histograms (bars) of the error magnitude

248 together with the best-fitting mixture-distribution models (lines). **c**, Average decision weights showing the

249 contributions of each presented motion direction to the decision.

250 As in Experiment 1, we next characterised the time-course of attentional selection

251 and decision-making by analysing the N2b and CPP, respectively. The ERP topography (Fig.

252 4a) in Experiment 2 was broadly consistent with that of Experiment 1, showing a bilateral

253 posterior negativity and a centro-medial positivity. The time-course of the N2b and CPP (Fig.

254 4b) followed closely the modulation of colour saturation, peaking sharply around 1.8 and

255 3.8 s and decaying quickly thereafter. There was a second modulation of both components,

broadly coinciding with the coherent motion onsets (ca. 2.5 and 4.5 s), which rose and fell more slowly than the colour-evoked components, most likely due to jittered timing of the motion onsets.

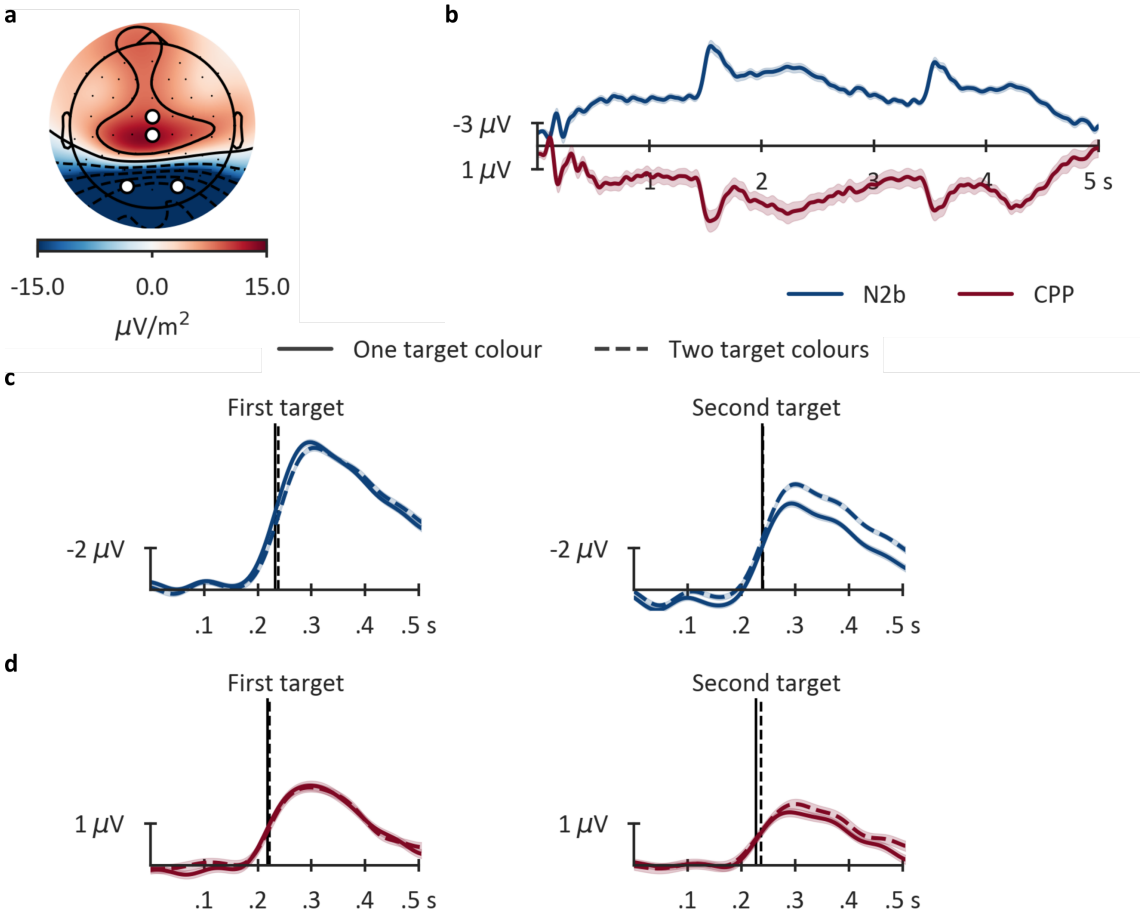

Figure 4. Time course of ERP correlates of attentional selection and decision making in Experiment 2. a, Surface-Laplacian-filtered EEG topography averaged across all conditions at the middle of peak colour saturation for both epochs (2 s and 4 s after dot onset). The markers denote electrode pairs [O1 and O2] and [CPz and Cz] which were used for computing the N2b and CPP, respectively. **b**, The N2b (blue trace) and the CPP (red) averaged across all experimental conditions for the total trial duration. Notice the difference between the voltage scale for the N2b and CPP time-traces. **c**, Time-course of the N2b during the gradual increase in colour saturation, shown separately per epoch and experimental condition. **d**, Time-course of the CPP during the same period. Conventions as in Figure 2.

Mimicking the behavioural serial order effect, the N2b onset latency (Fig. 4c) was somewhat shorter for the first epoch than for the second (235 and 240 ms, $F_{c(1,30)} = 4.10$, $p = .052$). Similarly, the N2b slopes were steeper and the peak N2b amplitude was higher in the first epoch than in the second (slopes: -61.50 and -45.47 μV/s, $F_{c(1,30)} = 21.13$, $p < .001$, amplitudes: 1.95 and 1.41 μV, $F_{c(1,30)} = 88.31$, $p < .001$). While for the first epoch, there were no differences in the peak N2b amplitude for the one- and two-target conditions ($t_c < 1$), for the second epoch, the peak N2b amplitude was higher for two-target than for one-target colour trials (-5.17 and -4.28 μV, $t_{c(1,30)} = 3.30$, $p = .002$). Similar to the N2b findings, analyses of the CPP (Fig. 4d) revealed a shorter onset latency (220 and 231 ms, $F_{c(1,30)} = 5.04$, $p = .032$), a marginally steeper slope (17.57 and 13.34 μV/s, $F_{c(1,30)} = 3.23$, $p = .083$) and a higher peak amplitude (1.95 and 1.42 μV, $F_{c(1,30)} = 6.40$, $p = .017$) for the first epoch relative to the second. Increasing attentional demands had a marginally significant effect on the peak CPP amplitude (1.62 and 1.57 μV, for one- and two target colours, respectively, $F_{c(1,30)} = 4.01$, $p = .054$) which was due to a higher peak amplitude for two target colours relative to one in the second epoch ($t_{c(1,30)} = 2.30$, $p = .029$). Overall, the ERP analyses of Experiment 2 replicated the most salient findings of Experiment 1. First, the ERP time-course mirrored the behavioural order effect and, second, an increase in attentional demands increased the peak amplitudes, albeit only in the second epoch.

To independently characterise target and distractor processing, we next analysed the amplitude of SSVEP responses elicited by the frequency-tagged motion stimuli. There was a strong (≈2 dB, Fig. 5b), frequency-specific response which peaked at the Oz electrode over the occipital pole (Fig. 5a).

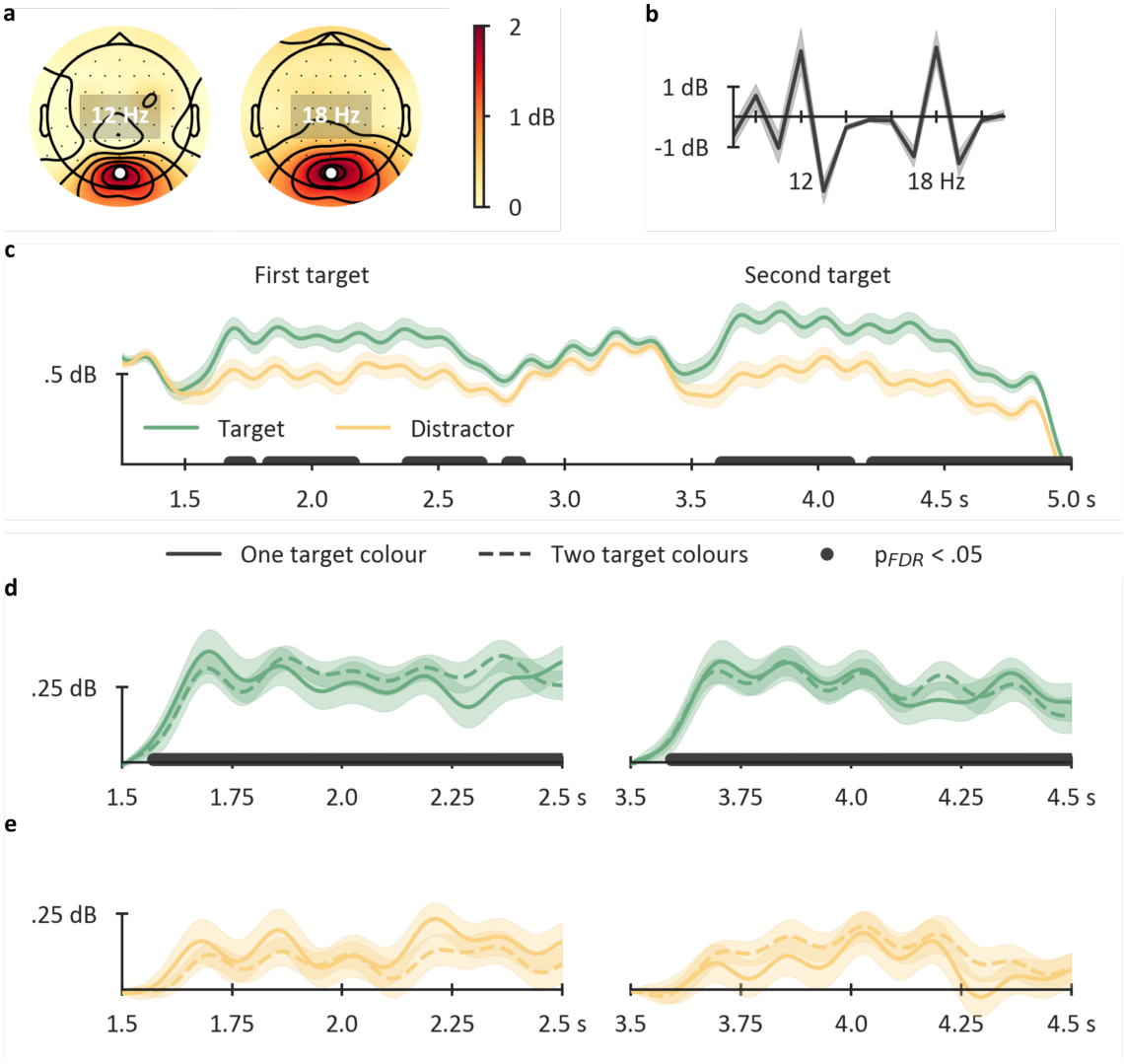

Figure 5. Time-course of target and distractor processing measured as SSVEP power in Experiment 2. a, Topography of the total power at 12 Hz and 18 Hz normalized relative to the neighbouring frequencies, computed using a fast-Fourier transform during periods of maximal colour saturation (1.5–2.5 s, and 3.5–4.5 s). **b**, Normalized total SSVEP power (M ± 95% CI) at Oz electrode during the period of maximal colour saturation averaged across epochs and all experimental conditions. **c**, Time-resolved target- and distractor-evoked SSVEP for the whole trial duration averaged across all experimental conditions (M ± 1 within-participants SEM). Black dots denote times at which the difference between target and distractor power was significant at $p_{FDR\text{-}corrected} < .05$. **d**, Target-evoked SSVEPs per epoch and per experimental condition baseline-corrected relative to the trough power in the -50–50 ms window around the peak colour saturation (1.5 s and

3.5 s for the first and the second epochs, respectively). **e**, Distractor-evoked baseline-corrected SSVEPs per epoch and experimental condition.

Time-frequency analyses revealed that the power was similar for target and distractor patches (Fig. 5c) prior to the increase in colour saturation in both the first epoch and the second. This suggests that participants divided attention across both patches during periods in which the two patches were indistinguishable. As the colour saturation increased, there was a transient *decrease* in power for the two patches in both the first epoch (ca. 1.5 s) and the second (ca. 3.5 s). Whereas the power for target patches in both epochs (Fig. 5d, grey dots) recovered quickly, the respective power for distractor patches remained at the same (decreased) level throughout the epochs (Fig. 5e), yielding a robust effect of task-relevance (average power: .24 and .10 dB for target and distractor patches, respectively, $F_{1,30} = 11.64$, $p = .002$, $\eta_p^2 = .28$). Finally, the SSVEP power was comparable for the first and second epoch, and for the one- and two-target colour conditions (all $F \leq 1.25$, all $p \geq .272$).

The transient decrease in power at the epoch onset (Fig. 5c) may reflect a gating mechanism described in computational models of neuronal firing rates (Purcell *et al.*, 2010, 2012). In the absence of a stimulus, such gating prevents neuronal noise from reaching a decision threshold by accident. Presenting a stimulus (in this case, increasing colour saturation) would initially strengthen the gating, which might take time to overcome and result in a transient decrease in power. A comparable decrease in power for both target and distractor patches suggests that attentional selection does not modulate the gating. The degree to which different patches were able to escape the gating, however, was strongly influenced by task-relevance.

322 Taken together, the results of Experiment 2 suggest that, following initial
323 suppression of both target and distractor signals, attention selectively boosts task-relevant
324 target signals, but leaves task-irrelevant, distractor signals relatively unaffected. Consistent
325 with the behavioural decision weights, the SSVEP analyses revealed that participants
326 successfully selected targets and disregarded distractors, despite the fact that the two dot
327 patches were spatially overlapped at fixation.

328 *Discussion*

329 The central goal of the present study was to characterise the behavioural and neural
330 processes associated with complex decision-making. Unlike simple decision-making (Gold
331 and Shadlen, 2007; Forstmann, Ratcliff and Wagenmakers, 2016; Ratcliff *et al.*, 2016), our
332 complex decision-making task involves selective processing of target signals in the presence
333 of distractors and requires integration of several, independent decisions into a single,
334 'complex' decision. Although one could think of many other attributes of complex decision-
335 making, here we focused on these two specifically as we could characterise them readily
336 using the standard dot-motion assay of decision-making. The behavioural results of
337 Experiments 1 and 2 demonstrated that complex decision-making relies almost solely on
338 task-relevant sensory input, even when a similar but task-irrelevant signal is concurrently
339 presented. Since most previous studies on decision-making used only task-relevant stimuli,
340 the present study adds to the literature by demonstrating a profound influence of selective
341 attention on visual decision-making.

342 The averaging task that we developed permitted us to characterise integration of
343 independent decisions into one, complex decision. We found that complex decisions are

biased for sequential visual presentations, such that participants weight more heavily the first of two successive target stimuli. As the two signals had identical, supra-threshold motion coherence, differences in sensory processing of the first and the second epoch cannot account for the order effect. Neither can a simple process of memory decay explain the order effect, as this would predict stronger decision weights for the *second*, more recent epoch, than the first. The sequential order bias we observed here echoes the "robust averaging" effect reported in studies that require averaging of more than two signals (Gardelle and Summerfield, 2011; Li *et al.*, 2017; Spitzer, Waschke and Summerfield, 2017). In these tasks, stimuli that are similar to the grand average of all presented stimuli carry greater weight than dissimilar stimuli. It is unlikely, however, that the order effect we observed in the present study reflects robust averaging as the two target signals in our task were, by design, equally informative. Instead, the order effect we observed suggests the existence of a distinct, higher-level mechanism specifically involved in complex decision-making.

In Experiment 1, analyses of a neural correlate of evidence accumulation, the CPP ERP, revealed higher peak amplitude in epochs with target-coloured signals relative to no-target epochs. As colour was always task-relevant, our findings suggest that *the degree* to which task-relevant stimulus properties are processed depends on the match with the relevant target features. In combination with previous studies (Twomey, Kelly and O'Connell, 2016) which have found no CPP to completely task-irrelevant stimulus attributes (e.g., orientation), our findings demonstrate that evidence accumulation evolves from coarse stimulus representation (e.g., are the stimuli coloured or not?) to fine (e.g., are the

366 stimuli target- or distractor-coloured?). The fact that, in target-absent epochs, participants
367 were able to stop processing relatively quickly suggests that a decision can be made at
368 several levels of accumulated evidence, rather than after reaching a single, fixed decision-
369 threshold.

370 Finally, deciding about the motion direction of one or two possible target colours
371 mattered little for the CPP time-course in both Experiments 1 and 2. These results are of
372 particular importance for the decision-making literature. A critical distinction between
373 different evidence-accumulation models is whether they assume mutual inhibition between
374 different choices (Leite and Ratcliff, 2010) or independent evidence accumulation (Usher
375 and McClelland, 2001) across choice alternatives. The mutual inhibition architecture
376 predicts changes in decision-making dynamics as the number of choices increases. By cueing
377 our participants to attend to just one target colour or two colours we varied the number of
378 choice alternatives. By showing that the neural correlates of decision-making do not co-vary
379 with the number of choices – at least in the range of choice alternatives used in the present
380 study – our findings are consistent with the notion of independent evidence accumulation.

381 In Experiment 1, our index of the neural correlate of attentional selection (the N2b)
382 revealed a stronger response to task-relevant versus irrelevant stimuli. Likewise, in
383 Experiment 2 only target SSVEPs were modulated by visual attention, whereas the distractor
384 SSVEPs remained unaffected. These findings imply that the reason for participants' accurate
385 responses was effective attentional selection of task-relevant sensory input. Remarkably,
386 we also found that having participants maintain two attentional sets, as opposed to just
387 one, had no reliable influence on either behaviour or electrophysiological correlates of

attentional selection. Since target and distractor stimuli were always presented concurrently within a foveated and attended region of space, these findings go beyond recent work (Eimer and Grubert, 2014; Grubert *et al.*, 2017) which found that the time-course of spatial attention changes little as attentional demands increase. Whereas previous studies (Andersen, Hillyard and Müller, 2008; Andersen, Müller and Hillyard, 2015) using similar methods found that multiple stimulus features *across* different dimensions (e.g., colour and orientation) can be attended in parallel, the present study shows that multiple features *within* a single feature dimension (e.g., colour) can also be attended with little, if any, cost.

The motion averaging task we have introduced here has great potential as a tool for investigating the mechanisms underlying complex decision-making. Dynamic weighting of individual decisions is ubiquitous in daily life: for example, when deciding whether or not to cross a busy road. Our averaging paradigm captures both individual decisions and weighting components of complex decision-making in a straightforward and well characterised motion discrimination task. In our task, individual motion signals are uncorrelated and, considered in isolation, are not predictive of the final decision. Hence, the averaging task permits independent parameterisation of both *simple* and *complex* decision-making processes. Using neuroimaging methods with high spatial resolution such as fMRI, future studies could identify the brain areas involved in simple decision-making, on the one hand, and complex decision-making, on the other.

The integrative aspect of complex decision-making is particularly interesting. In the present study, we found that participants were biased such that they relied more strongly

410 on the first target epoch than the second. This finding suggests that integrating two simple
411 decisions into one, complex decision involves higher-level cognitive control processes.
412 Future studies could investigate determinants of decision biases in the averaging task: for
413 example, whether or not the order effect persists even when the two signals have different
414 coherence levels. As the averaging task can capture the integration process, using this task
415 to characterise complex decision-making across the lifespan or in clinical groups with
416 difficulties in cognitive control will shed light on the development of complex decision-
417 making abilities which are a hallmark of adaptive, intelligent behaviour.

418 *Methods*

419 **Participants.** Seventy-two healthy volunteers (39 females, average age 21.5 ± 2.5
420 years, 36 per experiment) participated in the study after providing written informed
421 consent. The sample size per experiment was estimated so that the statistical tests (t-test)
422 would have sufficient power (>= .80) to detect medium to strong effects (d >= .5). All
423 participants had normal or corrected-to-normal visual acuity and normal colour vision. In
424 Experiment 1, three participants were identified as outliers based on their behavioural
425 performance and/or EEG signals (see below for details). Data from five participants were
426 removed from Experiment 2, based on the same criteria, leaving 33 and 31 participants per
427 experiment, respectively. The study was approved by the Human Research Ethics
428 Committee of The University of Queensland, and was conducted in accordance with the
429 Human Subjects Guidelines of the Declaration of Helsinki.

430 **Stimuli, task and procedure.** In Experiment 1, participants were asked to monitor
431 the direction of successively presented epochs of coherent motion, and to indicate the

432 average direction of two target-motion events at the end of the trial using a response dial. A
433 response feedback symbol showing the correct answer was presented after every trial.

434 At the beginning of each trial, a central disk cued participants to look for one or two
435 target colours in the subsequent displays (Fig. 1a). This was followed by a buffer period
436 showing a field of 40 grey, randomly-moving dots. The dots' colour saturation gradually
437 increased (Fig. 1b) to reveal two overlapping, coloured-dot patches, before decreasing in
438 saturation and returning to grey. Each trial consisted of three such epochs – in two of these
439 epochs one of the two overlapping dot patches was rendered in the target colour, and the
440 other appeared in a distractor colour. Each trial contained two epochs in which a target was
441 present, and one epoch in which both dot patches were rendered in different distractor
442 colours (no-target epochs). Target patches were displayed equally often in the first, second
443 and third epochs of a trial. A single colour was cued in the first two blocks with a different
444 colour per block. In the remaining four blocks, two colours were cued. Between target-
445 present epochs, the target colours either repeated or changed equally often.

446 Dot-motion was generated at 40% coherence, with a speed of 19 dva/s, 100 ms dot-
447 life, different signal-dots across frames and random-walk noise-dots (Scase, Braddick and
448 Raymond, 1996). Note that we deliberately used a relatively high motion coherence value as
449 we wanted to measure participants' *average* decision to the two target events, rather than
450 their success in discriminating individual targets. Although coherent motion was present
451 throughout the epoch (1.5 s, Fig. 1b), different motion-directions were discernible only at
452 higher colour saturations. The motion directions were uniformly sampled from 0°–359°,
453 with the target-distractor and target-target difference remaining within 30°–150°. Five

easily distinguishable colours (Fig. 1b) were selected in the HSB colour-space with a minimum hue difference of 72° and medium saturation and brightness (50). Two randomly-selected colours served as targets and two as distractors. Participants completed 30 practice trials followed by six blocks of 44 trials (= 264 trials). Each experimental session lasted approximately one hour.

In Experiment 2, the field size, dot size and dot number were doubled relative to Experiment 1, to optimise the display for recording SSVEPs. The dot-motion was generated at 2.5 dva/s, with an infinite dot life. Three distinctive colours (maximum saturation 75, minimum colour separation 90°, Fig. 3a) were selected; two colours served as targets, and the remaining one served as a distractor. The distractor and target colours were counterbalanced across participants. Different dot patches were frequency-tagged (Norcia *et al.*, 2015) by flickering (ON-OFF) the patches at 12 Hz and 18 Hz. Different frequencies were randomly and equally often paired with target and distractor colours. The colour saturation increased rapidly (.25 s) from grey to full saturation, and remained at maximum saturation for 1 s. Only two epochs of coloured dots were shown, and both epochs within a trial contained a target-motion patch. Coherent motion events were presented for .5 s during the maximum saturation period, and at variable times (.25–.50 s after maximum colour saturation was reached). Participants completed 64 practice trials followed by six blocks of 64 trials (= 384 trials). All other details were the same as in Experiment 1.

Apparatus. The experiments were conducted in a dark, acoustically and electromagnetically shielded room. The stimuli were presented on a 24” monitor with 1920×1080 resolution and a refresh rate of 144 Hz. The experimental software was custom-

476 coded in Python using the PsychoPy (Peirce, 2007, 2009) toolbox. EEG signals were recorded
477 using 64 Ag-AgCl electrodes (BioSemi ActiveTwo) arranged in the 10-20 layout and sampled
478 at 1,024 Hz.

479 **Behavioural analyses.** To identify outlier participants, the distributions of error
480 magnitudes (i.e., the angular difference between the response and the correct answer)
481 were compared to a uniform distribution (i.e., pure guessing) using the Kolmogorov-Smirnov
482 test. Participants for whom the probability of the null hypothesis (i.e., a uniform distribution
483 of error magnitudes) exceeded .001 were removed from further analyses. The remaining
484 distributions per experimental condition and per participant were fitted to a theoretical
485 model (Schneegans and Bays, 2016), and responses were separated into noisy target
486 responses and random guesses. To quantify decision weights, a multiple-regression (OLS)
487 model with a term for each of the presented motion directions, expressed as complex
488 numbers, was fitted to the responses, separately per participant and experimental
489 condition. The absolute value of the resulting regression coefficients reflects the influence
490 of each of the presented coherent motion signals on the response, i.e., its *decision weight*.

491 **EEG analyses.** EEG signals were analysed using the MNE-Python (Gramfort *et al.*,
492 2013) toolbox. The data were offline re-referenced to the average electrode, low-pass
493 filtered at 99 Hz and notch-filtered at 50 Hz to eliminate line noise. The recorded signal was
494 pre-processed using the FASTER (Nolan, Whelan and Reilly, 2010) algorithm for automated
495 artefact rejection. The pre-processed signal was down-sampled to 256 Hz, segmented into
496 epochs between the cue-onset and the response-display onset, baseline-corrected relative
497 to -.1–0 s pre-trial and linearly de-trended. Outlier epochs and participants were identified

using the FASTER algorithm and removed from further analyses. The N2b and CPP ERPs were computed by averaging O1/O2 and Cz/CPz electrodes, respectively, across trials. Each motion epoch within a trial was extracted from the onset of the increase in colour saturation and baseline-corrected relative to a common baseline during -.1–0 s, averaged across all epochs. The peak N2b and CPP amplitudes were identified using the jackknife-method (Ulrich and Miller, 2001). Using the same method, ERP onset latencies were computed at 50% peak amplitude. The ERP slopes were computed as the amplitude difference between -.05 s and .05 s relative to the ERP onset, and divided by .1 s so as to yield μV/s. Time-resolved SSVEP power at tagged frequencies was computed using Morlet wavelets with fixed-width .5 s Gaussian taper, and normalized relative to the neighbouring frequencies. For analyses of the target (Fig. 5d) and distractor SSVEPs (Fig. 5e), the power per epoch was baseline-corrected relative to the mean power in the -.05–.05 s interval around the onset of maximal colour saturation (1.5 and 3.5 s, for the first and the second epoch, respectively). The mean power per epoch was computed during the 1 s of maximal colour saturation.

Acknowledgments

This work was supported by the Australian Research Council (ARC) Centre of Excellence for Integrative Brain Function (ARC Centre Grant CE140100007). JBM was supported by ARC Australian Laureate Fellowship (FL110100103).

References

Andersen, S. K., Hillyard, S. A. and Müller, M. M. (2008) 'Attention Facilitates Multiple Stimulus Features in Parallel in Human Visual Cortex', *Current Biology*, 18(13), pp. 1006–1009. doi: 10.1016/j.cub.2008.06.030.

Andersen, S. K. and Müller, M. M. (2010) 'Behavioral performance follows the time course of neural facilitation and suppression during cued shifts of feature-selective attention', *Proceedings of the National Academy of Sciences*, 107(31), pp. 13878–13882. doi: 10.1073/pnas.1002436107.

Andersen, S. K., Müller, M. M. and Hillyard, S. A. (2015) 'Attentional Selection of Feature Conjunctions Is Accomplished by Parallel and Independent Selection of Single Features', *Journal of Neuroscience*, 35(27), pp. 9912–9919. doi: 10.1523/JNEUROSCI.5268-14.2015.

Churchland, A. K. and Ditterich, J. (2012) 'New advances in understanding decisions among multiple alternatives', *Current Opinion in Neurobiology*. (Decision making), 22(6), pp. 920–926. doi: 10.1016/j.conb.2012.04.009.

Churchland, A. K., Kiani, R. and Shadlen, M. N. (2008) 'Decision-making with multiple alternatives', *Nature Neuroscience*, 11(6), pp. 693–702. doi: 10.1038/nn.2123.

Eimer, M. and Grubert, A. (2014) 'Spatial Attention Can Be Allocated Rapidly and in Parallel to New Visual Objects', *Current Biology*, 24(2), pp. 193–198. doi: 10.1016/j.cub.2013.12.001.

Forstmann, B. U., Ratcliff, R. and Wagenmakers, E.-J. (2016) 'Sequential Sampling Models in Cognitive Neuroscience: Advantages, Applications, and Extensions', *Annual Review of Psychology*, 67(1), pp. 641–666. doi: 10.1146/annurev-psych-122414-033645.

Gardelle, V. de and Summerfield, C. (2011) 'Robust averaging during perceptual judgment', *Proceedings of the National Academy of Sciences*, 108(32), pp. 13341–13346. doi: 10.1073/pnas.1104517108.

Gold, J. I. and Shadlen, M. N. (2007) 'The Neural Basis of Decision Making', *Annual Review of Neuroscience*, 30(1), pp. 535–574. doi: 10.1146/annurev.neuro.29.051605.113038.

Gramfort, A. *et al.* (2013) 'MEG and EEG data analysis with MNE-Python', *Frontiers in Neuroscience*, 7. doi: 10.3389/fnins.2013.00267.

Grubert, A. *et al.* (2017) 'Rapid top-down control over template-guided attention shifts to multiple objects', *NeuroImage*, 146(Supplement C), pp. 843–858. doi: 10.1016/j.neuroimage.2016.08.039.

Heekeren, H. R., Marrett, S. and Ungerleider, L. G. (2008) 'The neural systems that mediate human perceptual decision making', *Nature Reviews. Neuroscience*, 9(6), pp. 467–479. doi: 10.1038/nrn2374.

Kelly, S. P. and O'Connell, R. G. (2013) 'Internal and External Influences on the Rate of Sensory Evidence Accumulation in the Human Brain', *The Journal of Neuroscience*, 33(50), pp. 19434–19441. doi: 10.1523/JNEUROSCI.3355-13.2013.

Leite, F. P. and Ratcliff, R. (2010) 'Modeling reaction time and accuracy of multiple-alternative decisions', *Attention, Perception, & Psychophysics*, 72(1), pp. 246–273. doi: 10.3758/APP.72.1.246.

Li, V. *et al.* (2017) 'Robust averaging protects decisions from noise in neural computations', *PLOS Computational Biology*, 13(8), p. e1005723. doi: 10.1371/journal.pcbi.1005723.

Loughnane, G. M. *et al.* (2016) 'Target Selection Signals Influence Perceptual Decisions by Modulating the Onset and Rate of Evidence Accumulation', *Current Biology*, 26(4), pp. 496–502. doi: 10.1016/j.cub.2015.12.049.

Morey, R. D. (2008) 'Confidence intervals from normalized data: A correction to Cousineau', in *Tutorials in Quantitative Methods for Psychology , 4*, pp. 61–64.

Nolan, H., Whelan, R. and Reilly, R. B. (2010) 'FASTER: Fully Automated Statistical Thresholding for EEG artifact Rejection', *Journal of Neuroscience Methods*, 192(1), pp. 152–162. doi: 10.1016/j.jneumeth.2010.07.015.

Norcia, A. M. *et al.* (2015) 'The steady-state visual evoked potential in vision research: A review', *Journal of Vision*, 15(6), pp. 4–4. doi: 10.1167/15.6.4.

O'Connell, R. G., Dockree, P. M. and Kelly, S. P. (2012) 'A supramodal accumulation-to-bound signal that determines perceptual decisions in humans', *Nature Neuroscience*, 15(12), pp. 1729–1735. doi: 10.1038/nn.3248.

Peirce, J. W. (2007) 'PsychoPy—Psychophysics software in Python', *Journal of Neuroscience Methods*, 162(1–2), pp. 8–13. doi: 10.1016/j.jneumeth.2006.11.017.

Peirce, J. W. (2009) 'Generating Stimuli for Neuroscience Using PsychoPy', *Frontiers in Neuroinformatics*, 2. doi: 10.3389/neuro.11.010.2008.

Purcell, B. A. *et al.* (2010) 'Neurally Constrained Modeling of Perceptual Decision Making', *Psychological Review*, 117(4), pp. 1113–1143. doi: 10.1037/a0020311.

Purcell, B. A. *et al.* (2012) 'From Salience to Saccades: Multiple-Alternative Gated Stochastic Accumulator Model of Visual Search', *The Journal of Neuroscience*, 32(10), pp. 3433–3446. doi: 10.1523/JNEUROSCI.4622-11.2012.

Ratcliff, R. *et al.* (2016) 'Diffusion Decision Model: Current Issues and History', *Trends in Cognitive Sciences*, 20(4), pp. 260–281. doi: 10.1016/j.tics.2016.01.007.

Ratcliff, R., Philiastides, M. G. and Sajda, P. (2009) 'Quality of evidence for perceptual decision making is indexed by trial-to-trial variability of the EEG', *Proceedings of the National Academy of Sciences*, 106(16), pp. 6539–6544. doi: 10.1073/pnas.0812589106.

Scase, M. O., Braddick, O. J. and Raymond, J. E. (1996) 'What is Noise for the Motion System?', *Vision Research*, 36(16), pp. 2579–2586. doi: 10.1016/0042-6989(95)00325-8.

Schneegans, S. and Bays, P. M. (2016) 'No fixed item limit in visuospatial working memory', *Cortex*, 83(Supplement C), pp. 181–193. doi: 10.1016/j.cortex.2016.07.021.

Shadlen, M. N. and Kiani, R. (2013) 'Decision Making as a Window on Cognition', *Neuron*, 80(3), pp. 791–806. doi: 10.1016/j.neuron.2013.10.047.

Spitzer, B., Waschke, L. and Summerfield, C. (2017) 'Selective overweighting of larger magnitudes during noisy numerical comparison', *Nature Human Behaviour*, 1(8), p. 0145. doi: 10.1038/s41562-017-0145.

Summerfield, C. and Tsetsos, K. (2015) 'Do humans make good decisions?', *Trends in Cognitive Sciences*, 19(1), pp. 27–34. doi: 10.1016/j.tics.2014.11.005.

Treue, S., Hol, K. and Rauber, H.-J. (2000) 'Seeing multiple directions of motion—physiology and psychophysics', *Nature Neuroscience*, 3(3), pp. 270–276. doi: 10.1038/72985.

Tsetsos, K., Usher, M. and McClelland, J. L. (2011) 'Testing Multi-Alternative Decision Models with Non-Stationary Evidence', *Frontiers in Neuroscience*, 5. doi: 10.3389/fnins.2011.00063.

Twomey, D. M., Kelly, S. P. and O'Connell, R. G. (2016) 'Abstract and Effector-Selective Decision Signals Exhibit Qualitatively Distinct Dynamics before Delayed Perceptual Reports', *Journal of Neuroscience*, 36(28), pp. 7346–7352. doi: 10.1523/JNEUROSCI.4162-15.2016.

Ulrich, R. and Miller, J. (2001) 'Using the jackknife-based scoring method for measuring LRP onset effects in factorial designs', *Psychophysiology*, 38(5), pp. 816–827. doi: 10.1111/1469-8986.3850816.

Usher, M. and McClelland, J. L. (2001) 'The time course of perceptual choice: the leaky, competing accumulator model', *Psychological Review*, 108(3), pp. 550–592.

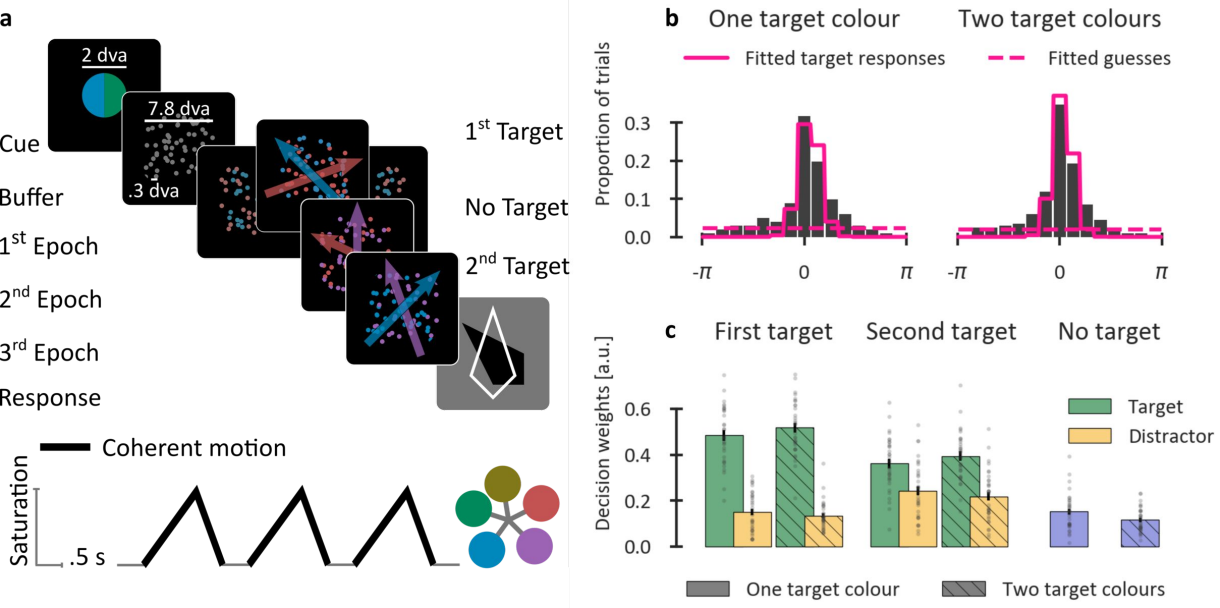
a
2 dva
7.8 dva
.3 dva
Cue
Buffer
1st Epoch
2nd Epoch
3rd Epoch
Response
1st Target
No Target
2nd Target
Coherent motion
Saturation
.5 s
b
One target colour
Two target colours
Fitted target responses
Fitted guesses
Proportion of trials
0.3
0.2
0.1
0.0
-π
0
π
c
First target
Second target
No target
Decision weights [a.u.]
0.6
0.4
0.2
0.0
Target
Distractor
One target colour
Two target colours

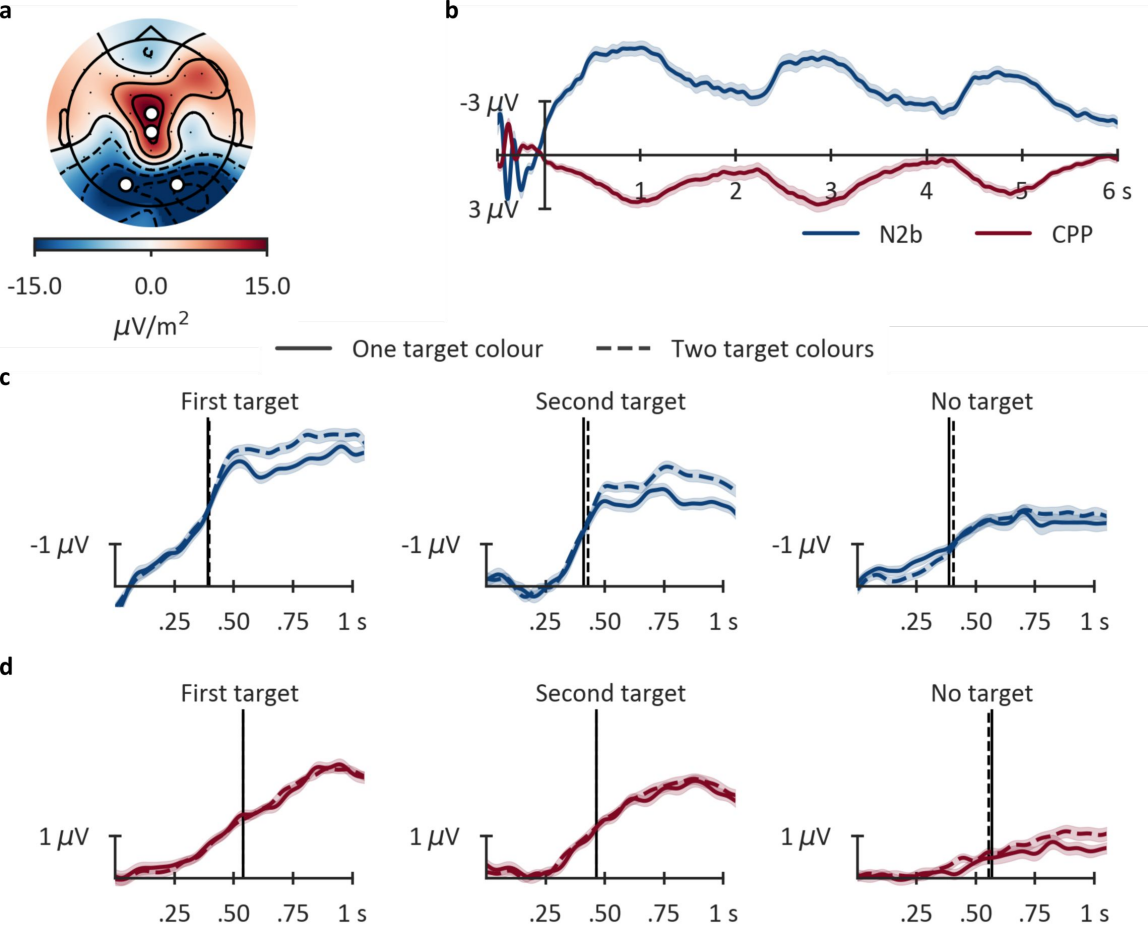
a
-15.0
0.0
15.0
μV/m²
b
-3 μV
3 μV
1
2
3
4
5
6 s
N2b
CPP
One target colour
Two target colours
c
First target
Second target
No target
-1 μV
.25
.50
.75
1 s
d
1 μV

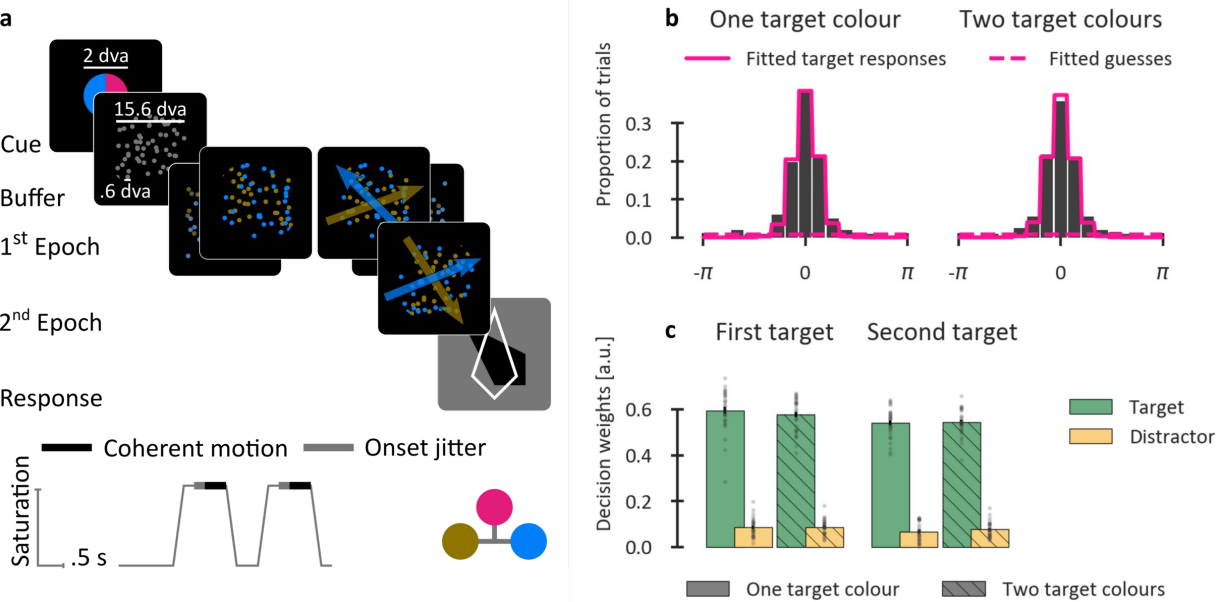
a
2 dva
15.6 dva
.6 dva
Cue
Buffer
1st Epoch
2nd Epoch
Response
Coherent motion
Onset jitter
Saturation
.5 s
b
One target colour
Two target colours
Fitted target responses
Fitted guesses
Proportion of trials
0.3
0.2
0.1
0.0
-π
0
π
c
First target
Second target
Decision weights [a.u.]
0.6
0.4
0.2
0.0
Target
Distractor
One target colour
Two target colours

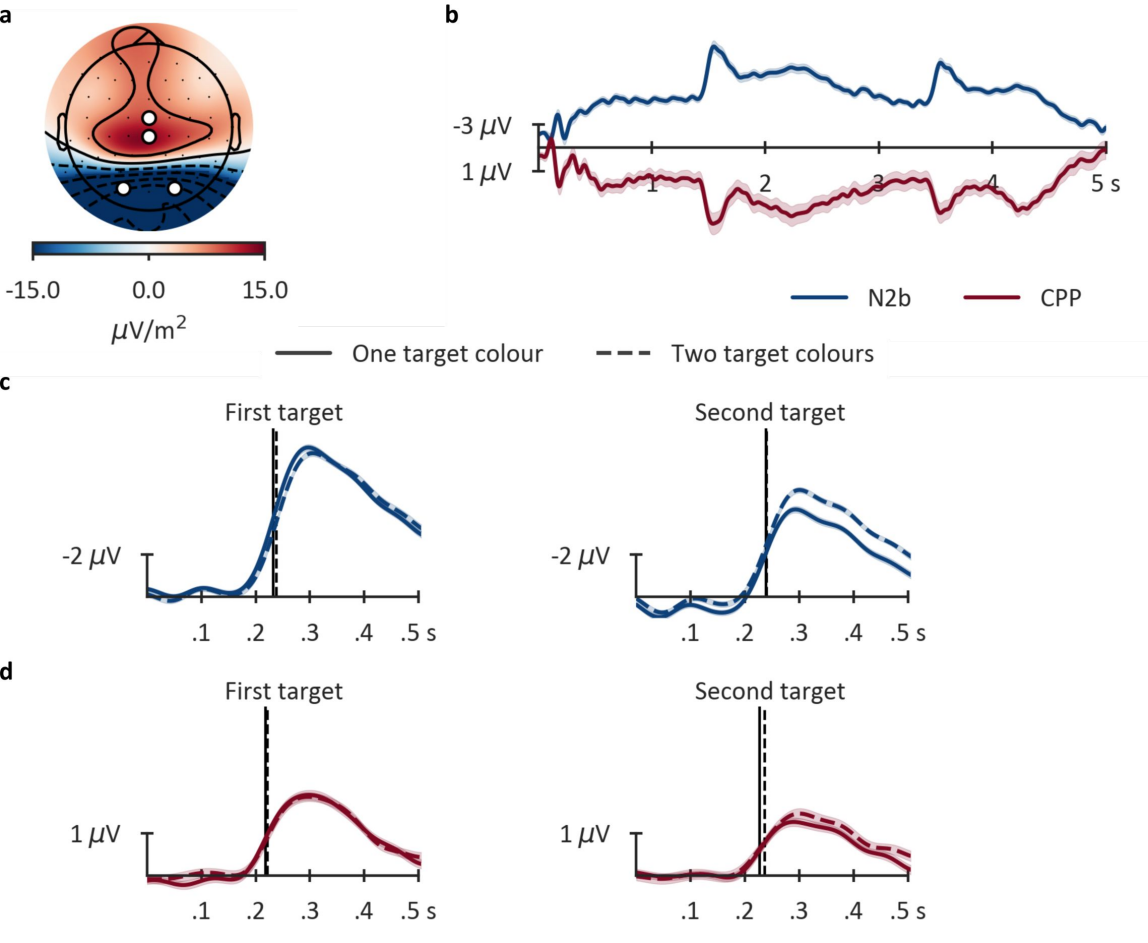
a
-15.0
0.0
15.0
μV/m²
b
-3 μV
1 μV
1
2
3
4
5 s
N2b
CPP
One target colour
Two target colours
c
First target
Second target
-2 μV
.1
.2
.3
.4
.5 s
d
1 μV

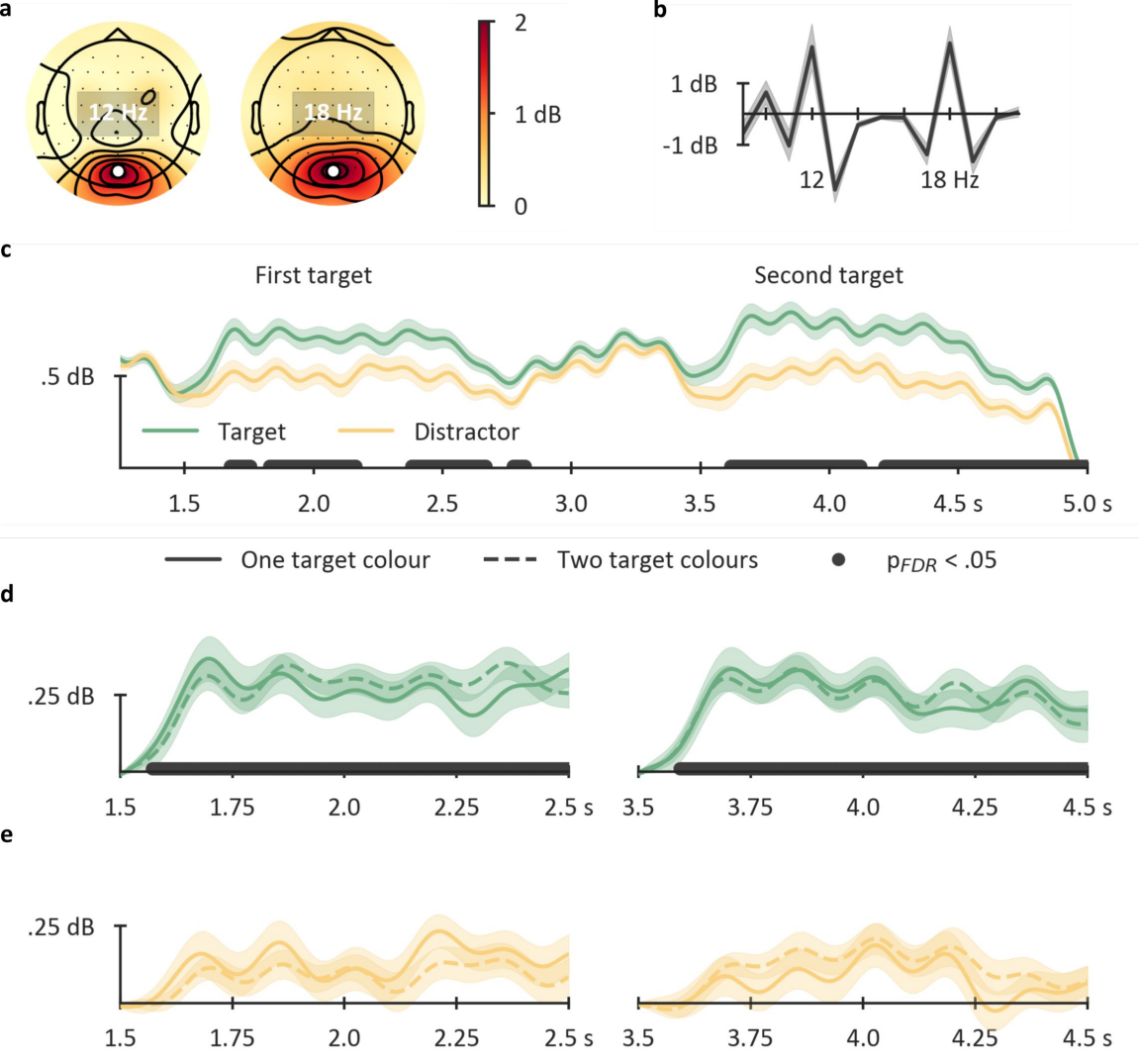
a
12 Hz
18 Hz
2
1 dB
0
b
1 dB
-1 dB
12
18 Hz
c
First target
Second target
.5 dB
Target
Distractor
1.5
2.0
2.5
3.0
3.5
4.0
4.5 s
5.0 s
One target colour
Two target colours
pFDR < .05
d
.25 dB
1.5
1.75
2.0
2.25
2.5 s
3.5
3.75
4.0
4.25
4.5 s
e
.25 dB
1.5
1.75
2.0
2.25
2.5 s
3.5
3.75
4.0
4.25
4.5 s